scientific reports

Check for updates

OPEN

Environmental enrichment alleviates neuropathic pain-associated anxiety by enhancing the function of parvalbumin interneurons in the anterior cingulate cortex

Zhuo-Yu Ren[1,5], Bao-Yu Han[1,2,5], Li-Yuan Zhao[1], Xue-Jie Lou[1], Yuan-Xiang Tao[3], Guang-Fen Zhang[4]✉ & Jian-Jun Yang[1]✉

Chronic neuropathic pain is often accompanied with comorbid anxiety. However, effective interventions for this anxiety are highly limited. This study aims to examine the effect of environmental enrichment (EE) on spared nerve injury (SNI)-induced neuropathic pain-associated anxiety behaviors and explore the mechanisms underlying this effect. EE effectively ameliorated anxiety-like behaviors followed by SNI. EE also significantly reversed the phenotypic loss of parvalbumin (PV) interneurons in the anterior cingulate cortex (ACC) and impaired gamma oscillations under SNI-induced neuropathic pain conditions. In addition, EE reversed the SNI-induced reduction in the number of PV puncta around Ca^{2+}/calmodulin-dependent protein kinase II-positive neurons. Furthermore, enhancing the function of PV interneurons could effectively improve the SNI-caused anxiety-like behaviors. In contrast, the inhibition of PV interneurons led to anxiety-like behaviors in naïve mice. Our findings suggest that EE significantly improves anxiety-like behaviors under neuropathic pain conditions, likely by enhancing the function of PV interneurons in ACC.

Keywords Environmental enrichment, Neuropathic pain, PV interneurons, Gamma Oscillation

Neuropathic pain is often accompanied with many comorbid symptoms, in which anxiety is the most common. Anxiety often further aggravates neuropathic pain and thus forms a vicious circle between pain and anxiety, resulting in the increased burden in the treatment of these disorders. About 50% of neuropathic pain patients reported anxiety-like symptoms, up to about 30% of whom have been diagnosed with an anxiety disorder[1,2]. Although the mechanisms underlying the anxiety under neuropathic pain conditions have been studied, there are still no effective treatments for neuropathic pain-associated anxiety[3]. Therefore, new and effective therapies for comorbid anxiety disorders following peripheral nerve injury are urgent to be developed. Environmental enrichment (EE) is an emerging strategy of nondrug treatment for mental diseases[4,5]. It is a low-cost, side-effect-free, and promising mitigation strategy for many mental disorders. More interestingly, EE has been shown to improve anxiety caused by social stress, sleep deprivation, and even Parkinson's disease[6–8]. However, it is unclear whether EE can prevent neuropathic pain-associated anxiety.

The anterior cingulate cortex (ACC) is one of the key brain regions that play a critical role in the mechanisms underlying neuropathic pain and associated comorbid anxiety[9]. The neurons in the ACC can be reliably activated in various neuropathic pain models[10]. Increased ACC neuronal excitability leads to nociceptive and anxiety-like behavioral responses following peripheral nerve injury[11], whereas decreased ACC neuronal excitability

[1]Department of Anesthesiology, Pain and Perioperative Medicine, The First Affiliated Hospital of Zhengzhou University, Zhengzhou, China. [2]Department of Anesthesiology, Jinan Children's Hospital, Jinan, China. [3]Department of Anesthesiology, New Jersey Medical School, Rutgers, The State University of New Jersey, Newark, USA. [4]Department of Anesthesiology, Shandong Provincial Hospital Affiliated to Shandong First Medical University, Jinan, China. [5]Zhuo-Yu Ren and Bao-Yu Han contributed equally to this work. ✉email: wfzhgf87@126.com; yjyangjj@126.com

significantly reduces abdominal hyperalgesia and anxiety in rats with pancreatitis[12]. These data suggest that abnormally increased ACC neuronal excitability plays an important role in the occurrence of neuropathic pain and related anxious behaviors. Therefore, this study examined whether EE improved the neuropathic-pain-associated anxiety behaviors likely through regulating the ACC neuronal excitability.

Parvalbumin (PV)-positive neurons account for about half of the GABAergic neurons in the cortex and are implicated in regulating neuronal excitability[13]. Recent studies reported the role of PV interneurons in regulating Alzheimer's disease-related anxiety and anxiety-like behaviors under chronic stress conditions in rodents[14,15]. However, whether PV-positive neurons participate in neuropathic pain-associated anxiety is still elusive. The present study was designed to explore the therapeutic effects of EE on neuropathic pain and its associated anxiety-like behaviors and to identify the key role of ACC PV interneurons in the EE-induced alleviation of anxiety-like behaviors under neuropathic pain conditions.

Methods

Animals

Adult male C57BL/6J mice weighing 22–26 g (8–12 weeks) were obtained from the SPF (Beijing) Biotechnology Co., Ltd. The animals were housed in a temperature- and humidity-controlled room (22 °C ± 2 °C) in a 12-h light/dark cycle with food and water available ad libitum. The experiments adhered to the Committee for Research and Ethical Issues of the International Association for the Study of Pain (IASP) and the National Research Council's Guide for the Care and Use of Laboratory Animals guidelines. All procedures were conducted in full compliance with the ARRIVE guidelines. In addition, all animals were euthanized with pentobarbital sodium (150 mg/kg) before obtaining tissue samples.

Mice were randomly divided into three groups: (1) in the sham group, mice only received sham surgery and standard environment; (2) in the spared nerve injury (SNI) group, mice received SNI surgery and standard environment; and (3) in the SNI + EE group, mice received SNI surgery and EE treatment.

To explore the effects of chemogenetic activation of PV interneurons on the behavior of SNI mice, the SNI model mice were randomly divided into (1) mCherry + VEH group; (2) mCherry + CNO group; (3) hM3Dq + VEH group; (4) hM3Dq + CNO group. To investigate the effects of chemogenetic inhibition of PV interneurons on the behavior of naïve mice, naïve mice were randomly divided into (1) mCherry + VEH group; (2) mCherry + CNO group; (3) hM4Di + VEH group; (4) hM4Di + CNO group.

SNI model establishment

To mimic clinical neuropathic pain, a previously established SNI mouse model was used in this study[16]. In brief, mice were deeply anesthetized by intraperitoneally injecting of sodium pentobarbital (60 mg/kg). Under aseptic surgical conditions, the left sciatic nerve branches were isolated through blunt dissection of the femoral biceps muscle. The peroneal and tibial nerves were both tightly ligated and transected distal to the ligation, with the intact sural nerve. The overlying muscles and skin were then sutured and sterilized postoperatively. Sham surgery was carried out with identical preceding procedures except for nerve ligation and transection.

Environmental enrichment (EE)

Yehezkel et al.'s protocol was used in our EE strategy[4]. Simply put and large polycarbonate cages (60 × 32 × 38 cm) were equipped with running wheels, toys, a maze-like tube system, houses and nesting batting. The configuration was changed every 2 days. Mice were maintained in this EE condition throughout the 5-week light and dark periods. The standard cages (29 × 18 × 16 cm) were used as a control.

Paw withdrawal threshold (PWT)

PWT to mechanical stimulation was examined by using the up-down method as described previously[17]. Briefly, the mice were placed inside a transparent plexiglass box on metal mesh and adapted for at least 30 min. The Von Frey filaments were taken and punctured vertically into the lateral plantar skin of the left hindlimb. The same position of each mouse was carefully stimulated. The interval of each stimulation was 2–3 min, lasting no more than 6 s. The paw quick withdrawal (lofting) with or without licking and shaking was considered as positive "X". If no response was seen, a negative "O" was marked. Following the method of Bonin Robert et al.[17], a sequence with a combination of "O" and "X" was obtained. Finally, the 50% foot-shrinking reaction threshold (g) was calculated according to the open-source program in the literature[18].

Paw withdrawal latency (PWL)

A radiant heat test was performed to assess thermal hyperalgesia using a plantar analgesia tester (Infrared Hot Spur Pain Meter, RWD). Briefly, the mice were placed on the glass pane, and the plantar surface was vertically heated by a 5 mm-diameter laser radiant heat source. PWL was averaged with three consecutive tests with at least 5 min interval. A cut-off value of 20 s was applied to avoid possible tissue damage[19].

Open-field test (OFT)

The open-field apparatus is a 50 × 50 × 50 cm box with an open top. Mice were placed in the center of the arena and recorded for 5 min by a ceiling-fixed video camera. The SMART 3.0 video-tracking software was used to record the time spent in the central area and the total distance of movement. The chamber was cleaned with 75% ethanol after each test.

Elevated plus maze test (EPMT)

The apparatus consisted of one central area (5 × 5 cm) and four arms (35 × 5 cm) and was elevated 75 cm above the floor. Two opposite arms were opened without a wall, whereas the other two were enclosed by high walls.

Testing was carried out in a dimly lit room with a 40 W bulb hung 60 cm above the central part of the maze. Mice were placed in the center square facing an open arm and were allowed to explore the maze for 5 min. The light intensity was about 165 lx. During the testing period, the number of open-arm entries and the time spent in open arms were recorded using SMART 3.0 video-tracking software. If the mice fell off the elevated maze, the mouse was removed from the study.

Novelty-suppressed feeding test (NSFT)

The test was performed in a black homemade box (50 × 50 × 50 cm) with 1 cm-thick bedding at the bottom. All mice were food-deprived for 24 h prior to testing with ad libitum access to water. At the time of testing, the arena was illuminated at 300 lux during testing, and a food pellet was placed on a piece of paper at the center of the box. Then, the mice were placed in a corner of the box, and the time when they first picked up and ate food was recorded. The latency to feed was recorded with a maximum time of 10 min. After the mice began to eat food, they were immediately transferred to their respective cages alone. Then, a 10-min food consumption test was conducted to rule out the effect of differences in appetite on feed latency.

Microelectrode implantation and local field potential recording and analysis

Mice were anesthetized with intraperitoneal injecting sodium pentobarbital (60 mg/kg) and mounted on a stereotaxic apparatus (RWD Life Science) in a flat skull orientation. To completely expose the skull, the muscle, fascia tissue, and periosteum were removed. After the skull alignment, three-dimensional coordinates of the ACC region (AP: + 0.7 mm; ML: ± 0.2 mm; DV: − 1.5 mm) were obtained from the mouse brain atlas[20]. After a 3 × 3 mm cranial window was drilled in the skull, the cortex was fully exposed. A four-channel microelectrode used in our experiment was made of 35 μm nichrome alloy with a spacing of 300 μm. The electrode was slowly moved downward through the hole until the predetermined position was reached. The hole was closed with paraffin, and the electrode was fixed on the skull surface with dental acrylic cement. After waking up, the mice were placed in their original cages.

After a 1-week recovery under the original environmental conditions, the basal local field potential (LFP) was recorded in the home cage. A digital preamplifier (Plexon Inc., Dallas, TX) was used to transmit the signals, which were then digitized at a sampling rate of 40 kHz. During the recording session, all other electric appliances were turned off to prevent interference. A specific workstation running professional electrophysiological analysis software was used for data processing. For the LFP analysis, wideband recordings were down-sampled at 1250 Hz. In our study, the bands were filtered as follows: slow gamma, 30–50 Hz; medium gamma, 50–80 Hz; and fast gamma, 80–140 Hz. NeuroExplorer 5 (Plexon Inc., Dallas, TX) was used for all data analyses.

Viral injection

Briefly, mice were intraperitoneally injected with 60 mg/kg of sodium pentobarbital and then restrained in a stereotaxic apparatus (RWD Life Science). The skulls were fully exposed to locate bregma and lambda and drilled using a dental drill (WPI, OmniDrill35) at the target location. For chemogenetic manipulations, rAAV-fPV-Cre-bGH polyA (titer, 2.64×10^{12} vg/ml) and rAAV-EF1α-DIO-hM3Dq-mCherry-WPRE (titer, 2.72×10^{12} vg/ml) were premixed at a ratio of 1:1 for the specific activation of PV interneurons; rAAV-fPV-CRE-bGH polyA (titer, 2.64×10^{12} vg/ml) and rAAV-EF1α-DIO-hM4Di-mCherry-WPRE (titer, 2.72×10^{12} vg/ml) were premixed at a 1:1 ratio for the specific inhibition of PV interneurons; rAAV-fPV-Cre-bGH polyA and rAAV-Ef1α-DIO-mCherry-WPRE-hGH polyA were mixed in a 1:1 ratio to serve as the control virus group. A 200 nl volume of the virus was injected into the ACC (AP: +0.7 mm, ML: ±0.2 mm, DV: − 1.5 mm) with a Hamilton syringe (needle gauge 31) connected with a micro-syringe pump controller (WPI, USA) at a rate of 20 nl/min. Thereafter, the needle was held for an additional 5 min and then slowly withdrawn to allow diffusion. Finally, the skin was sewn back together. A 4-week expression was allowed for all viruses for maximum results. Clozapine-N-oxide (CNO, 2 mg/kg, Wuhan Brain TVA) was dissolved in 0.5% DMSO (dimethyl sulfide, Sigma) to activate or inhibit the PV interneuron function (the CNO group). The solvent control group only used the vehicle solvent without adding CNO (the mCherry + VEH group or hM3Dq / hM4Di + VEH group). All viruses and drugs used in this study were provided by Wuhan BrainTVA Co., Ltd.

Immunofluorescence examination

Mice were anesthetized by intraperitoneally injecting 60 mg/kg of sodium pentobarbital, transcardially perfused by phosphate buffer saline (PBS) followed by 4% paraformaldehyde (PFA) in 0.1 M phosphate buffer (pH 7.4) on postoperative day 38. The brain was collected and post-fixed in the 4% PFA overnight and dehydrated in 20% and 30% sucrose at 4 °C overnight. Then 25 μm-thick coronally sections of the ACC were collected. After being blocked with 10% normal goat serum in PBS for 1 h at room temperature, the sections were incubated with primary antibodies including mouse anti-Ca^{2+}/calmodulin-dependent protein kinase IIα (CaMKIIα; 1:1000, Abcam) and rabbit anti-PV (1:500, Abcam) in 10% normal goat serum plus PBS at 4 °C overnight. After being washed with PBS for 4 × 5 min, the sections were exposed to the secondary antibody goat anti-rabbit (1:500, Proteintech) or goat anti-mouse (1:500, Proteintech) for 1 h at room temperature. A fluorescence microscope (Olympus, FV1000) was used to capture fluorescent images with fluorescence intensity calculated by ImageJ Software. When fluorescence intensity was compared, the same exposure parameters are used in all sections. Additionally, the number of PV was determined using manual counting with the Cell Counter plugin in ImageJ-Fiji software. To analyze the PV puncta surrounding CaMKII α-positive cells, NIS-Elements Viewer and ImageJ software were utilized[21]. Specifically, the NIS-Elements Viewer was used to separate the red (CaMKII) and green (PV) channels. Subsequently, the background noise of the images was reduced using the "Subtract Background" function in ImageJ, with a rolling ball radius set to 50 pixels. Finally, only the PV puncta that exhibited 100% overlap with the CaMKII signal were quantified.

Statistical analysis

All statistical analyses were performed using GraphPad Prism for Windows version 8.0. All data were presented as mean and standard error (mean ± SEM). The Shapiro–Wilk test was performed to determine the normality for the parametric test. Student's t-test was conducted to examine differences between two groups, while two-way analysis of variance followed by the Bonferroni post hoc test was used to examine the difference between multiple groups. If the data does not meet the normal distribution and has equal variance, non-parametric tests should be used. A statistically significant difference was defined as a two-sided p-value < 0.05.

Results

EE effectively reduced anxiety-like behaviors in neuropathic pain mice

Figure 1A shows the flow chart of the experimental design. No significant differences in weights of the mice were seen among three groups during the observation period (Fig. 1B; $p > 0.05$). Compared with the sham group, PWT and PWL in the SNI group and SNI + EE group were significantly lower on days 7, 14, 21, 28, and 35 post surgery ($p < 0.001$, Fig. 1C-D). No significant difference was observed between the SNI group and SNI + EE group. These results indicate that EE treatment may not affect the SNI-induced mechanical allodynia and thermal hyperalgesia. In the OFT, the movement track of mice was shown in Fig. 1E. No significant differences were observed in the total distance traveled among three groups ($p > 0.05$, Fig. 1F). As expected, the mice in the SNI group spent less time in the central area compared with that in the sham group ($p < 0.01$, Fig. 1G). However, EE significantly blocked the SNI-induced reduction in the time spent in the central area ($p < 0.05$, Fig. 1G). Similarly, in the EPMT, the movement trajectory of mice was shown in Fig. 1H. No significant differences were observed in the total distance traveled by mice among three groups ($p > 0.05$, Fig. 1I). As predicted, compared with the sham group, mice in the SNI group had a significant reduction in time spent in open arms ($p < 0.05$, Fig. 1J). However, EE significantly attenuated the SNI-induced reduction in the duration spent in the open arms ($p < 0.05$, Fig. 1J). In the NFST (Fig. 1K), compared with the sham group, the latency time to feed was significantly increased in the SNI group ($p < 0.01$, Fig. 1L). EE significantly reduced the latency time of SNI mice to feed ($p < 0.05$, Fig. 1L). No significant difference was observed in the amount of food intake among three groups ($p > 0.05$, Fig. 1M). Taken together, our findings indicate that EE exerts an improving effect on neuropathic pain-associated anxiety.

Effect of the EE on the SNI-induced reductions of PV-positive interneurons in ACC

Figure 2A shows a representative image of immunofluorescence. The immunofluorescence results depicted that the number of PV-positive interneurons in the ACC region was significantly reduced in the SNI group compared with that in the sham group ($p < 0.001$, Fig. 2B). Moreover, the relative fluorescence intensity of PV-positive neurons in ACC was also markedly reduced in the SNI group comparing with the sham group ($p < 0.05$, Fig. 2C). Interestingly, The EE treatment blocked the SNI-induced reductions in number of PV-positive neurons ($p < 0.05$, Fig. 2B), but there was no significant difference in relative fluorescence intensity ($p > 0.05$, Fig. 2C).

Effect of the EE on the SNI-induced decrease in fast gamma in the PV neurons of ACC

PV interneurons regulate the synchronization of excitatory neurons through producing gamma oscillations[13]. Gamma oscillation was recorded and analyzed in awake, freely moving mice to further evaluate the role of PV interneurons in the anxiety-like symptoms after SNI. Figure 3A revealed the power spectral density in the ACC, and Fig. 3B displayed representative images of the local field potential. Figure 3C depicted the power spectral density curve. Power spectral analysis demonstrated that fast gamma power was significantly decreased in the SNI group when compared to the sham group ($p < 0.05$, Fig. 3D). This decrease was reversed after EE treatment (fast gamma, $p < 0.05$, Fig. 3D). Interestingly, there are no significant differences in medium gamma and low gamma among three groups ($p > 0.05$, Fig. 3E-F).

Effects of the EE on the SNI-induced reduction in the number of PV puncta around CaMKIIα-positive neurons in ACC

Figure 4A illustrates the representative immunofluorescence double-stained images of CAMKIIα and PV. The results showed that the number of PV puncta around the CaMKIIα cells in the SNI mice was significantly decreased than that in the sham group ($p < 0.001$, Fig. 4B). This decrease was not seen after EE treatment in the SNI mice ($p < 0.001$, Fig. 4B).

Chemogenetic activation of PV interneurons alleviated anxiety-like behaviors in neuropathic pain mice

Figure 5A–B illustrate the flow chart of the experimental design and viral injection diagram. The specificity of the virus was examined first. The immunofluorescence results identified the cells with mCherry signals in the ACC (Fig. 5C), which were highly co-localized with PV-positive cells (Fig. 5D). These double-labeled neurons (overlap of PV^+ and $mCherry^+$ cells) accounted for about 76.8% of the total PV positive cells, and for about 80.0% of the total mCherry positive cells (Fig. 5E). The PWT and PWL in all four groups were significantly decreased 7, 14, 21, 28, and 35 days after SNI surgery compared with baseline (Fig. 5F-G). In the OFT (Fig. 5H), no differences in the total distances were observed among four groups ($p > 0.05$, Fig. 5I). However, compared with the mCherry + CNO and hM3Dq + VEH groups, mice in the hM3Dq + CNO group spent significantly longer time exploring the center area during OFT ($p < 0.05$, Fig. 5J). In the EPMT (Fig. 5K), no significant difference in the total distance was observed among four groups ($p > 0.05$, Fig. 5L). However, compared with the mCherry + CNO and hM3Dq + VEH groups, the mice in hM3Dq + CNO group spent significantly more time in the open arm ($p < 0.001$, Fig. 5M). In the NSFT, the latency time of feeding was significantly shorter in the hM3Dq + CNO group than in the mCherry + CNO and hM3Dq + VEH groups ($p < 0.001$, Fig. 5N). However,

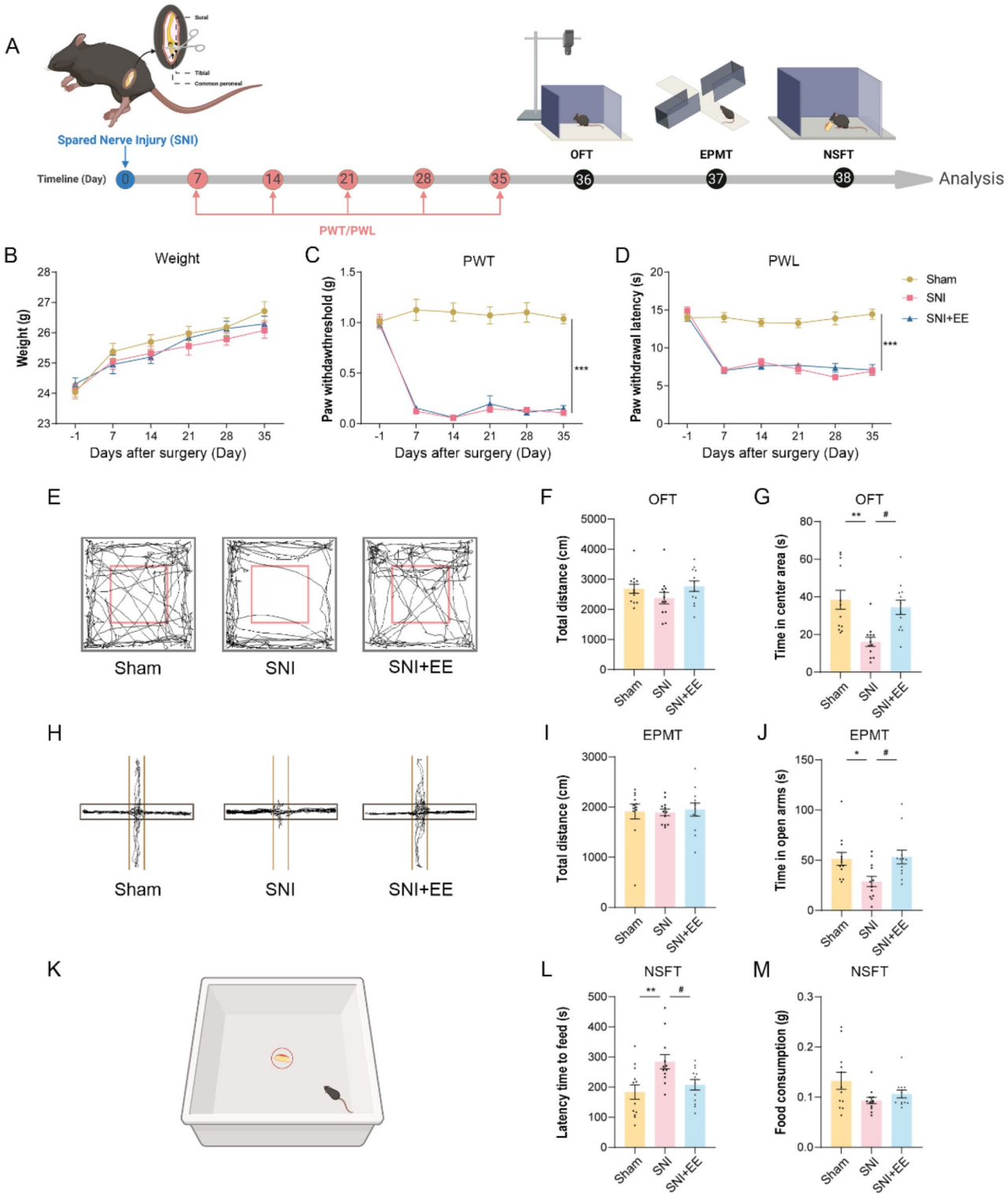

Fig. 1. Environmental enrichment effectively reduced anxiety-like behaviors in mice with neuropathic pain (**A**) Schematic of the experimental timeline (Created with bioRender.com). (**B**) Body weight monitoring during the experiment. (**C**) Paw withdrawal threshold to mechanical stimulation in the plantar test. (**D**) Paw withdrawal latency to heat stimulation in the plantar test. (**E**) Trajectories of mice in the OFT. (**F**) Total distance traveled throughout the area in the OFT. (**G**) Time spent in the central area of the OFT. (**H**) Trajectories of mice in the EPMT. (**I**) Total distance in the EPMT. (**J**) Time spent in open arms in the EPMT. (**K**) Schematic of novelty-suppressed feeding test. (**L**) Latency to initiate feeding in the NSFT. (**M**) Food consumption in the NSFT. All data represent the mean ± SEM ($n = 12$ mice per group). $^{*}p < 0.05$, $^{**}p < 0.01$, $^{***}p < 0.001$ versus the sham group; $^{\#}p < 0.05$ versus SNI group.

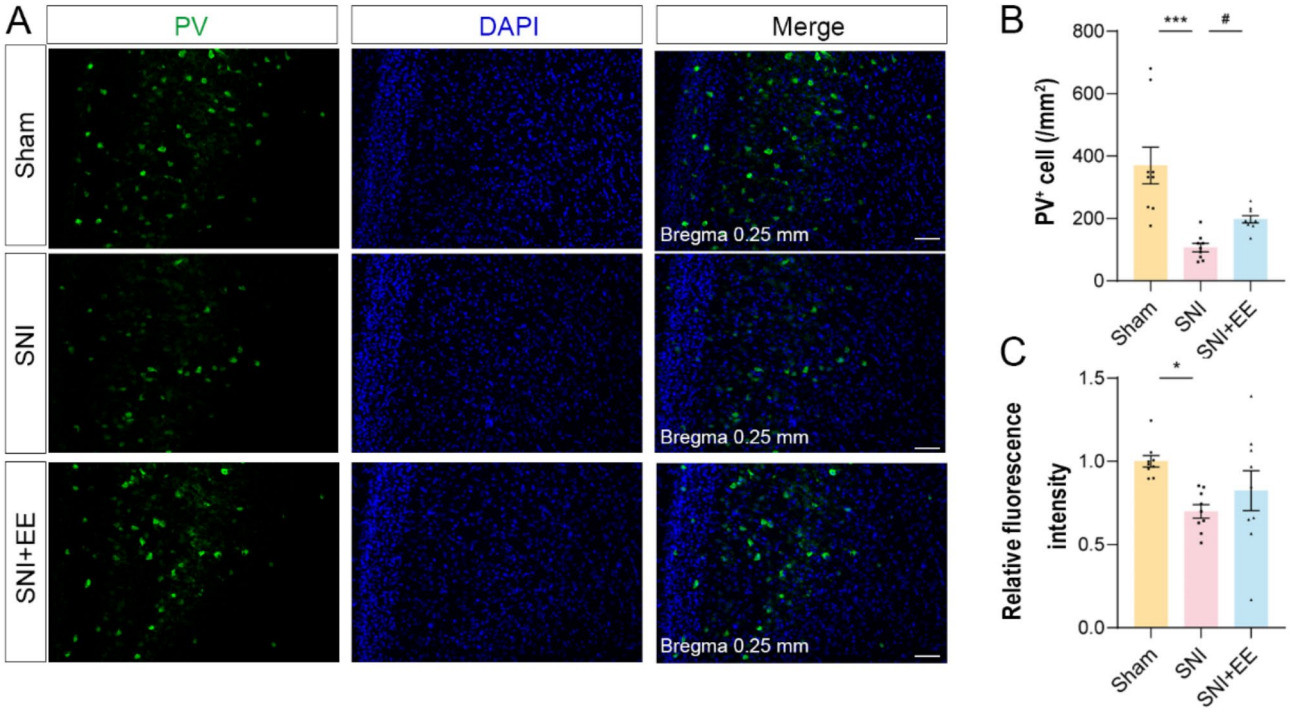

Fig. 2. The phenotypic loss of PV interneurons in the ACC induced by SNI is alleviated by EE (**A**) Representative images of PV-positive cells in the ACC in different groups of mice. (**B**) Quantitative results of the number of PV-positive cells contained in the image per square millimeter. (**C**) Quantitative results of relative fluorescence intensity of PV-positive cells under the same photographic parameters. Scale bars: 50 μm. All data represent the mean ± SEM ($n = 9$ sections from 3 mice per group). $^{*}p < 0.05$, $^{***}p < 0.001$ vsersus the sham group; $^{\#}p < 0.05$ versus SNI group.

food consumption did not show significant differences among four groups ($p > 0.05$, Fig. 5O). These findings indicate that enhancing the function of PV interneurons in ACC ameliorates the SNI-associated anxiety-like behaviors.

Chemogenetic Inhibition of PV interneurons increased anxiety-like behaviors in Naïve mice

To further examine whether PV interneuron function was sufficient for anxiety-like behaviors in mice, we examined the effects of inhibiting PV neuron function. The experimental design and the location of viral injection were shown in Fig. 6A–B. The viral specificity was shown in Fig. 6C–D. The double labeled cells (overlap of PV^{+} and $mCherry^{+}$) were accounted for about 74.3% of the total PV-positive cells, and for about 81.4% of the total mCherry-positive cells (Fig. 6E). The chemogenetic inhibition of PV function had no significant effect on basal PWT and PWL in naïve mice ($p > 0.05$, Fig. 6F–G). In the OFT (Fig. 6H), no significant differences in the total distance were observed among four groups ($p > 0.05$, Fig. 6I). Compared with the mCherry + CNO and hM4Di + VEH groups, mice in the hM4Di + CNO group spent significantly less time exploring the central region during OFT ($p < 0.001$, Fig. 6J). In the EPMT (Fig. 6K), no significant difference in total distance was observed among four groups ($p > 0.05$, Fig. 6L). However, compared with the mCherry + CNO and hM4Di + VEH groups, the hM4Di + CNO mice spent significantly less time in open arms ($p < 0.001$, Fig. 6M). In the NSFT, the latency time to food was significantly longer in the hM4Di + CNO group than in the mCherry + CNO and hM4Di + VEH groups ($p < 0.05$, Fig. 6N). However, the food consumption was not significantly different among four groups ($p > 0.05$, Fig. 6O). These data indicate that the inhibited function of PV interneurons may lead to anxiety-like behaviors in naïve mice.

Discussion

In this study, we demonstrated that the 5-week EE can reduce anxiety-like behaviors associated with neuropathic pain. In addition, these anxiety-like behaviors may be related to functional inhibition of PV interneurons in ACC. Therapeutic effect of EE on neuropathic pain-associated anxiety may be mediated through enhancing the function of PV interneurons in ACC.

Our results revealed that EE significantly improved anxiety-like behaviors after SNI, as evidenced by increased exploration time in the central region of OFT and extended exploration time in the open arm of the EPMT in SNI mice. However, in the pain behavioral test, our results showed that EE did not affect the SNI-induced mechanical allodynia and thermal hyperalgesia. This result contradicts the previous report, which showed that EE attenuated nerve injury-induced hypersensitivity to mechanical and cold stimuli[22]. This previous work used a model of neurological damage for up to 3 months followed by 2 months of environmental

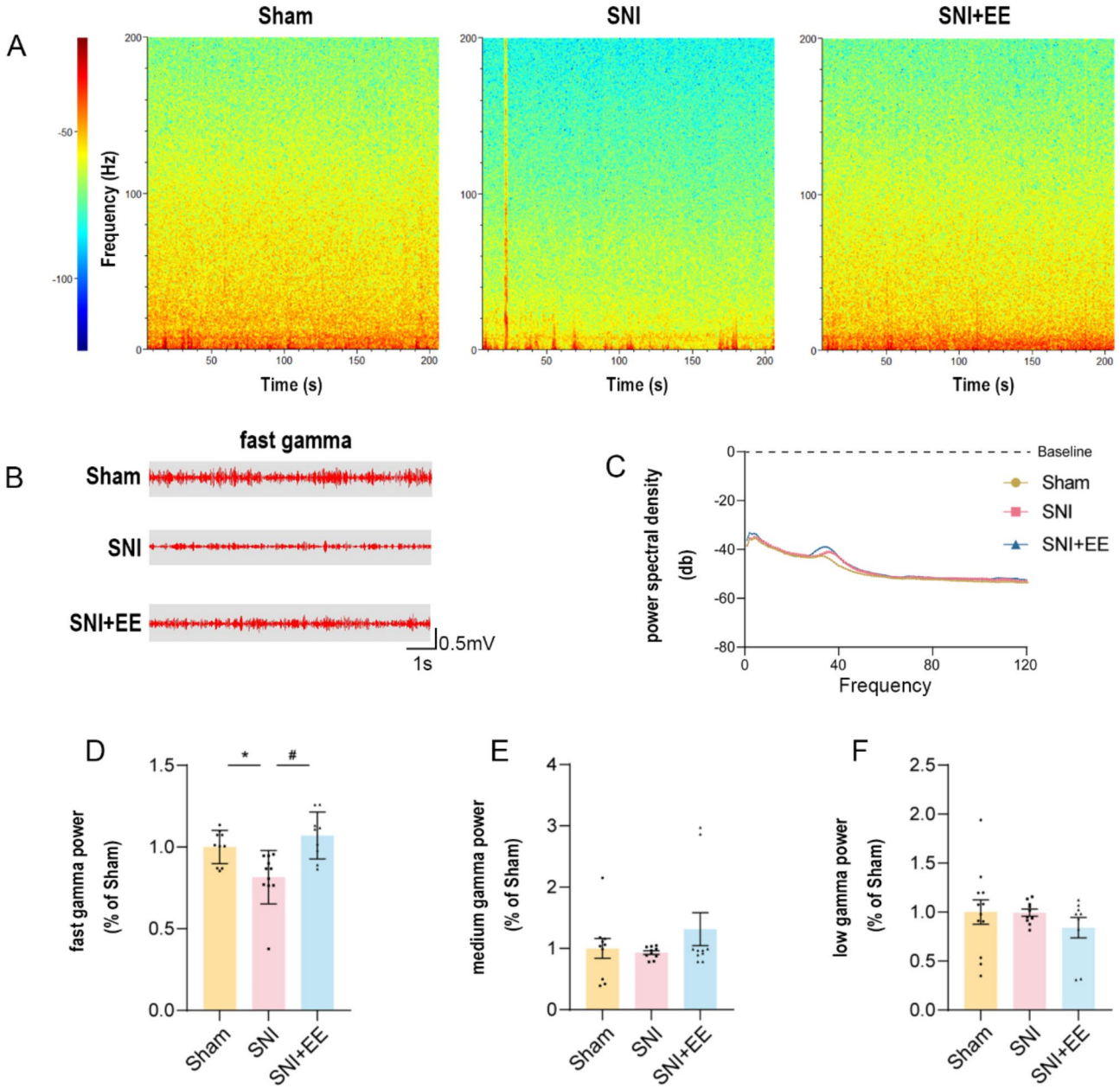

Fig. 3. EE improved the gamma oscillations of PV interneurons in ACC of mice with neuropathic pain-associated anxiety (**A**–**B**) Representative trace of neural oscillations and power spectral density. (**C**) Power spectral density analysis of the basal LFP. (**D**–**F**) Quantification of fast/medium/low gamma power in different groups. Data are presented as the mean ± SEM ($n = 9$–12 mice per group). $^{*}p < 0.05$, versus the sham group, $^{\#}p < 0.01$, versus SNI group.

manipulation. In contrast, the present study simultaneously performed pain behavioral tests and environmental manipulation within 35 days after SNI. These differences in timing and duration of intervention may account for the different therapeutic effects of EE on mechanical allodynia. A previous study reported that different EE programs were effective in reducing anxiety, but they may have the distinct effects on neuropathic pain[23]. Simple EE (only receiving three different objects) did not improve mechanical and cold stimuli hyperalgesia, whereas enhanced EE (receiving five different objects) completely abolished neuropathic pain. Different EE paradigms may have different potential effects on neuropathic pain. Moreover, recent studies have found that EE does not improve CFA-induced pain[24]. Therefore, whether EE can effectively relieve hyperalgesia in different pain models is still controversial. Future studies should further explore the effects of EE on nociceptive responses and the possible underlying mechanisms based on different pain models. Although the present study did not examine the effects of EE on mice in the sham group, our previous work has demonstrated no marked effect of EE on basal behavioral responses[21,25].

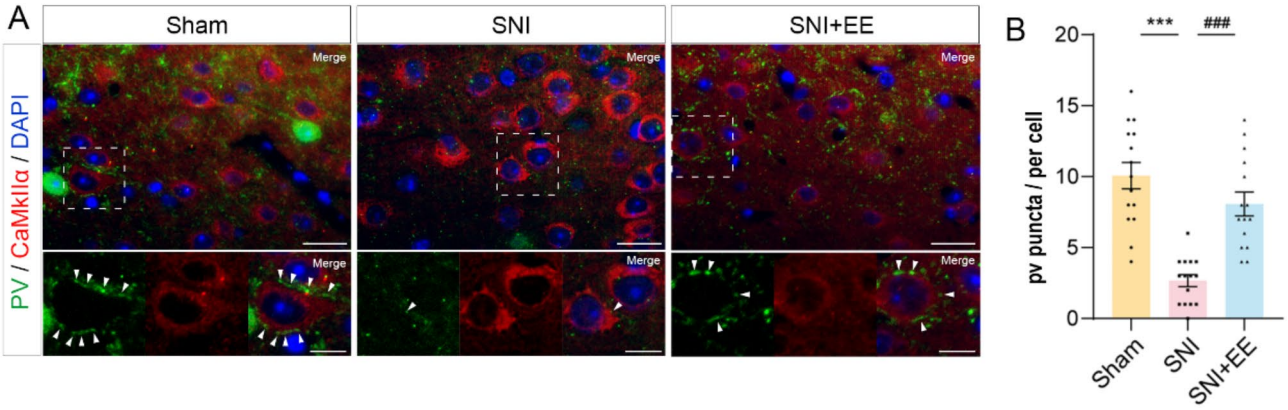

Fig. 4. Effects of EE on CaMKII-positive neurons and pericellular PV points in ACC of mice with neuropathic pain-associated anxiety (**A**) Representative immunofluorescence images of anti-CaMKIIα and anti-PV co-staining. (**B**) Quantitative analysis of PV puncta around CaMKII-positive cells. The scale of the overall image is 20 μm, and the scale of the local enlarged image is 10 μm. Data are presented as the mean ± SEM ($n = 15$ CaMKII cells from 3 mice per group). $^{***}p < 0.001$, versus the sham group, $^{###}p < 0.001$ versus the SNI group.

The balance between neuronal excitation and inhibition is required for maintaining normal brain function. The loss of this balance may be implicated in neuropathic pain and its accompanying emotional disorders[26]. Preclinical studies have reported that inhibitory interneuron disorders led to anxiety or depressive behaviors in chronic pain animals[23,27,28]. Our research team focused on the function of PV interneurons, the main subtypes of GABAergic interneurons, in ACC and explored their role in generating neuropathic pain -related anxiety in mice. Our immunofluorescence results showed that SNI decreased the number of PV-positive cells in ACC, consistent with that of previous reports[29]. Notably, chronic inflammatory pain induced by CFA led to a loss of both bilateral PV- and SOM-positive cells in ACC[30].Moreover, there were significant reductions in anxiety-like behaviors in chronic inflammatory pain rats after activating PV interneurons[30]. Hence, we focused on the effects of PV interneuron function on anxiety-like behaviors under neuropathic pain conditions. By activating or inhibiting PV interneurons in ACC through pharmacogenetics, we found that the activation of PV interneurons can improve neuropathic pain-associated anxiety-like behaviors. Consistently, inhibition of PV interneurons induced anxiety-like behaviors in naïve mice. In addition, the PV interneuron as inhibitory neurons exerted its physiological function mainly by regulating peripheral excitatory neurons. Our immunofluorescence results also revealed that the PV puncta regulating CaMKII, a marker of glutaminergic neurons in the forebrain, was significantly reduced in mice after SNI. This reduction may further enhance the glutaminergic neuronal activity in ACC. Interestingly, previous studies revealed that the overactivity of excitatory neurons in ACC might contribute to neuropathic pain genesis[31,32]. Our results further support the idea that glutaminergic neuronal hyperexcitability in ACC is a potential causative factor leading to anxiety-like behaviors in neuropathic pain mice and that this hyperexcitability may be partially attributed to the decreased function of PV interneurons.

Gamma oscillations are considered to be an important electrophysiological form that is closely related to the activity of PV neurons, in which inhibitory interneurons regulate the information integration of excitatory neurons[33]. However, how SNI affects gamma oscillations in the brain is still unclear. Here, we demonstrated that SNI significantly reduced the fast gamma oscillation power in ACC neurons. A previous study found that gamma oscillations in the primary somatosensory cortex (S1) were significantly increased during acute pain and were positively correlated with pain intensity[34]. However, another previous study reported that gamma oscillations were weakened during chronic pain[35]. Therefore, more relevant experiments should be designed to explore this controversy. In addition, present study did not observe significant changes in the medium and low gamma oscillations. Given that low gamma may be involved in visual processing and that medium gamma may be associated with memory and cognition[36,37], our analysis suggests that these two types of gamma oscillations may not be primarily involved in processing neuropathic pain and associated mood disorders.

Our study indicates that the ameliorating effect of EE on neuropathic pain-associated anxiety-like behaviors may be achieved by improving PV interneuron function in ACC. EE has been reported to improve the function of PV interneurons. A previous study showed that EE improved posttraumatic stress disorder by increasing the number of PV interneurons in the hippocampus[38]. In addition, EE can also promote the increased PV interneurons in stroke mice and improve the recovery of symptoms poststroke[39]. These results indicate that EE has great potential to improve the function of PV interneurons. Indeed, the data we provided support the central role of the PV interneuron function in ACC in regulating neuropathic pain-associated anxiety. EE as a potential alternative strategy leads to the resilience of neuropathic pain animals to anxiety through enhancing the PV interneuronal activity in ACC. Recent studies have reported that EE can improve anxiety by inhibiting the reduction of PV-positive interneurons in the medial prefrontal cortex caused by separation from the mother early in life[40]. These data further indicate that EE plays a therapeutic role in neuropathic pain-associated anxiety likely through enhancing the function of PV interneurons. This may provide a theoretical basis for developing treatment options of neuropathic pain-associated anxiety with low side effects in the future.

Interestingly, manipulating PV neurons only altered the anxiety-like behavior induced by neuropathic pain, without improving the pain-induced nociceptive responses. Studies have shown that in mice with neuropathic pain, there is a cortical excitatory/inhibitory imbalance, where the activity of SOM and PV neurons is reduced, and the activity of pyramidal neuron is increased. Activation of SOM neurons significantly improved the mechanical threshold reduction caused by neuropathic pain, while activation of PV neurons did not improve the mechanical threshold[41]. This finding suggests that PV neurons are likely more involved in the emotional component of pain, whereas SOM neurons are more involved in nociceptive perception. This difference may be related to the following: (1) PV cells mainly reside at peripheral synapses and have minimal regulation on dendritic Ca2 + spikes; (2) PV cells may provide transient inhibition to pyramidal cell bodies[42], while SOM cells exhibit high levels of spontaneous activity to inhibit the apical dendrites of pyramidal neurons[43]. In conclusion, further research is needed to explore the roles of different types of interneurons in pain.

This study also has several limitations. First, although our findings indicate that EE alleviates anxiety-like behaviors associated with neuropathic pain by activating PV interneurons in the ACC, the specific molecular mechanisms underlying the activation of PV interneurons remain unclear. Future research is needed to further explore the molecular mechanisms involved in the activation of PV interneurons. Additionally, we found that ACC interneurons may exert their effects through the modulation of excitatory glutamatergic neurons; however, the potential changes in excitatory neurons and excitatory synapses within the ACC are still not well understood. More importantly, the signaling mechanisms underlying these changes require further investigation. Finally, our study primarily focused on the anterior cingulate cortex due to its reliable activation during pain and its role in modulating pain-related anxiety-like behaviors[44,45]. However, the hippocampus, amygdala, and insula have also been reported to be involved in the occurrence of anxiety-like behaviors to some extent[46,47], and changes in these regions were not examined in the current study. Future research should further investigate the hippocampus, amygdala, and insular cortex to determine whether the effects of EE on inhibitory neurons are selective for the ACC. This study focused on male mice to align with historical comparators in the SNI neuropathic pain literature[48,49]. However, emerging evidence suggests there are significant gender differences in pain perception. Future work should systematically evaluate EE effects in female rodents across estrous stages to assess translational generalizability. Although our findings highlight ACC PV interneurons as a primary target of EE, future studies should map EE-induced changes in PV networks across the insula, hippocampus, and sensory cortices.

Conclusion

This study demonstrated that the decreased function of PV interneurons in ACC may be involved in anxiety-like behaviors under neuropathic pain conditions and reported that EE improved anxiety-like behaviors associated with neuropathic pain by enhancing the PV interneuron functions in ACC (Fig. 7). Present study provides the evidence of a nonpharmacological treatment strategy against anxiety-like behaviors in neuropathic pain mice. EE is a promising approach for restoring network homeostasis between excitability and inhibition of neurons in rodents, protecting the brain from the overactivation of ACC excitatory neurons caused by neuropathic pain, and may have potential applications in treating neurological disorders in humans.

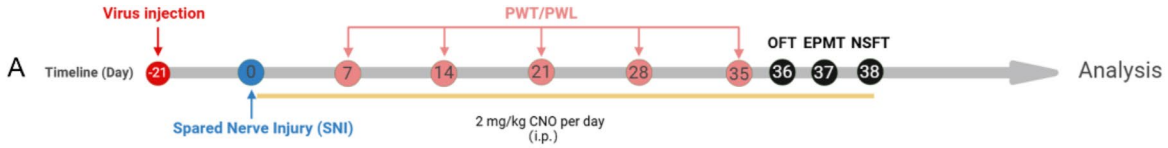
A
Virus injection
PWT/PWL
OFT EPMT NSFT
Timeline (Day)
-21
0
7
14
21
28
35
36
37
38
Analysis
Spared Nerve Injury (SNI)
2 mg/kg CNO per day
(i.p.)

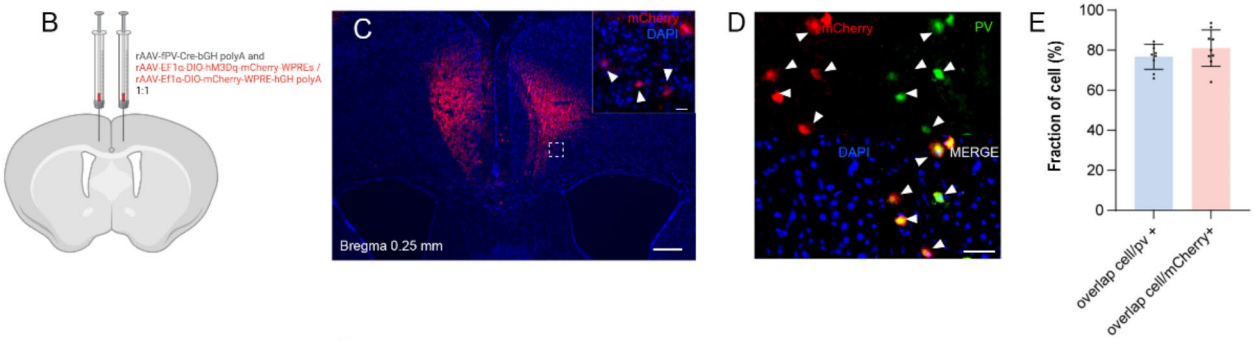
B
rAAV-fPV-Cre-bGH polyA and
rAAV-EF1α-DIO-hM3Dq-mCherry-WPREs /
rAAV-Ef1α-DIO-mCherry-WPRE-hGH polyA
1:1
C
mCherry
DAPI
Bregma 0.25 mm
D
mCherry
PV
DAPI
MERGE
E
Fraction of cell (%)
overlap cell/pv +
overlap cell/mCherry+

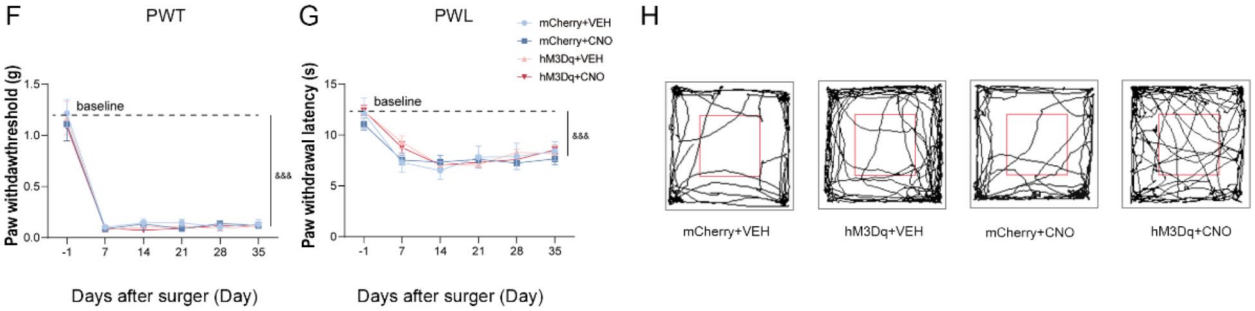
F
PWT
Paw withdawthreshold (g)
baseline
&&&
Days after surger (Day)
G
PWL
mCherry+VEH
mCherry+CNO
hM3Dq+VEH
hM3Dq+CNO
Paw withdrawal latency (s)
baseline
&&&
Days after surger (Day)
H
mCherry+VEH
hM3Dq+VEH
mCherry+CNO
hM3Dq+CNO

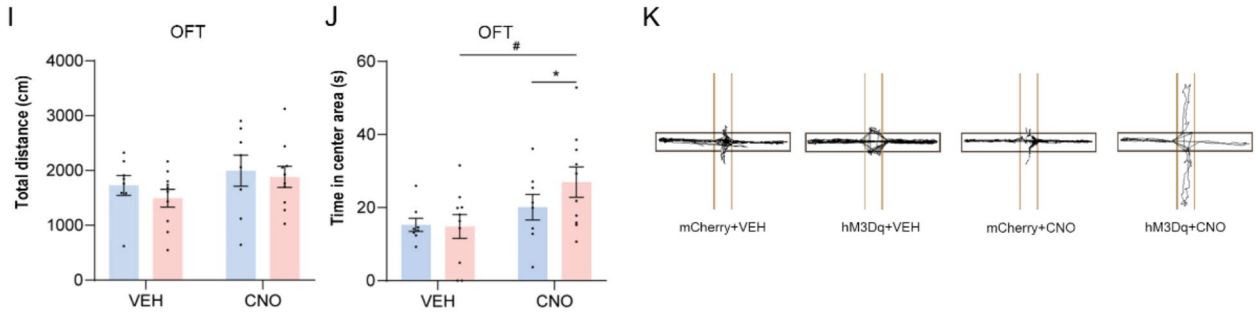
I
OFT
Total distance (cm)
VEH
CNO
J
OFT
#
*
Time in center area (s)
VEH
CNO
K
mCherry+VEH
hM3Dq+VEH
mCherry+CNO
hM3Dq+CNO

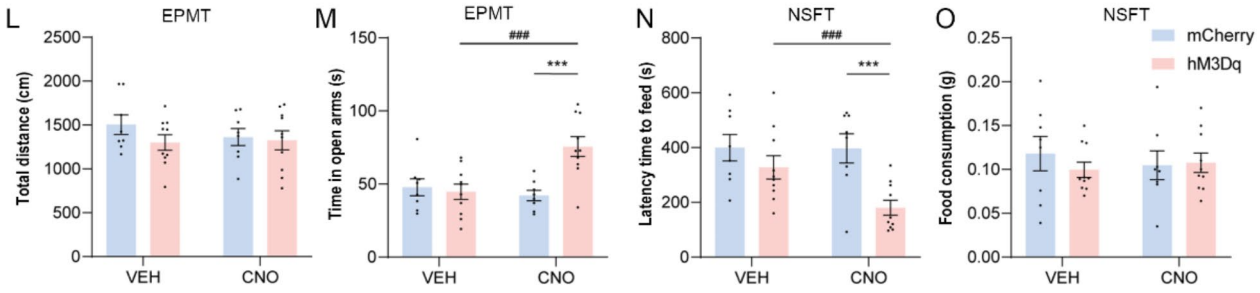
L
EPMT
Total distance (cm)
VEH
CNO
M
EPMT
###
***
Time in open arms (s)
VEH
CNO
N
NSFT
###
***
Latency time to feed (s)
VEH
CNO
O
NSFT
mCherry
hM3Dq
Food consumption (g)
VEH
CNO

◀**Fig. 5**. Chemogenetic activation of PV interneurons alleviated anxiety-like behaviors in mice with neuropathic pain (**A**) Schematic of the experimental design. (**B**) Diagram of viral microinjection. (**C**) Representative image showing the mCherry expression in the ACC (whole figure scale bars: 200 μm, local figure scale bars: 20 μm). (**D**) Representative images of PV interneurons (green) merged with mCherry (red) in the ACC (scale bars: 20 μm). (**E**) Quantitative analysis of the proportion of overlapping cells in total PV^+ cells, and the proportion of overlapping cells in total $mCherry^+$ cells. (**F**–**G**) Time courses showing paw withdrawal thresholds to von Frey filaments and withdrawal latency to heat stimulation. (**H**) Trajectories of mice in the OFT. (**I**) Total distance traveled throughout the arena in the OFT. (**J**) The time spent in the central area of the OFT. (**K**) Trajectories of mice in the EPMT. (**L**) Total distance traveled throughout the arena in the EPMT. (**M**) Time spent in the open arm in the EPMT. (**N**) Latency to initiate feeding in NSFT. (**O**) Food consumption in NSFT. All data represent the mean ± SEM ($n = 8$–10 mice per group). $^{\&\&\&}p < 0.001$ versus baseline; $^{*}p < 0.05$, $^{***}p < 0.001$ versus mCherry + CNO group; $^{\#}p < 0.05$, $^{\#\#\#}p < 0.001$ versus hM3Dq + VEH group.

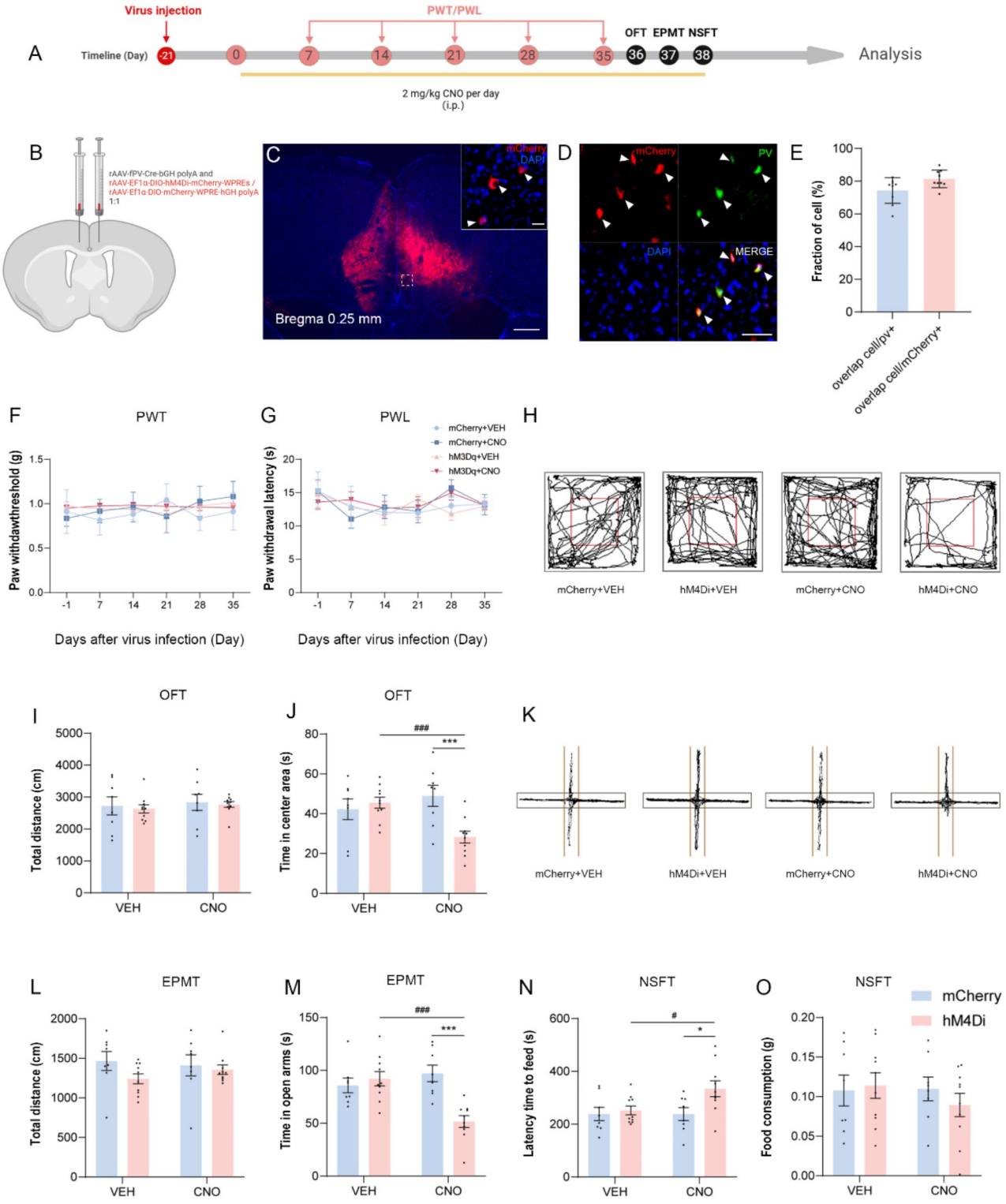
A
Virus injection
PWT/PWL
OFT EPMT NSFT
Timeline (Day)
-21
0
7
14
21
28
35
36
37
38
Analysis
2 mg/kg CNO per day
(i.p.)
B
rAAV-fPV-Cre-bGH polyA and
rAAV-EF1α-DIO-hM4Di-mCherry-WPREs /
rAAV-Ef1α-DIO-mCherry-WPRE-hGH polyA
1:1
C
mCherry
DAPI
Bregma 0.25 mm
D
mCherry
PV
DAPI
MERGE
E
Fraction of cell (%)
overlap cell/pv+
overlap cell/mCherry+
F
PWT
Paw withdawthreshold (g)
Days after virus infection (Day)
G
PWL
Paw withdrawal latency (s)
Days after virus infection (Day)
mCherry+VEH
mCherry+CNO
hM3Dq+VEH
hM3Dq+CNO
H
mCherry+VEH
hM4Di+VEH
mCherry+CNO
hM4Di+CNO
I
OFT
Total distance (cm)
VEH
CNO
J
OFT
Time in center area (s)
###
***
VEH
CNO
K
mCherry+VEH
hM4Di+VEH
mCherry+CNO
hM4Di+CNO
L
EPMT
Total distance (cm)
VEH
CNO
M
EPMT
Time in open arms (s)
###
***
VEH
CNO
N
NSFT
Latency time to feed (s)
#
*
VEH
CNO
O
NSFT
mCherry
hM4Di
Food consumption (g)
VEH
CNO

◂**Fig. 6**. Chemogenetic inhibition of PV interneurons caused anxiety-like behaviors in naïve mice (**A**) Schematic of the experimental design. (**B**) Diagram of virus microinjection. (**C**) Representative image showing the mCherry expression in the ACC (whole figure scale bars: 200 μm, local figure scale bars: 20 μm). (**D**) Representative images of PV interneurons (green) merged with mCherry (red) in the ACC (scale bars: 20 μm). (**E**) Quantitative analysis of the proportion of overlapping cells in total PV^+ cells, and the proportion of overlapping cells in total $mCherry^+$ cells. (**F–G**) Time courses showing paw withdrawal thresholds to von Frey filaments and withdrawal latency to heat stimulation. (**H**) Trajectories of mice in the OFT. (**I**) Total distance traveled throughout the arena in the OFT. (**J**) Time spent in the central area of the OFT. (**K**) Trajectories of mice in the EPMT. (**L**) Total distance traveled throughout the arena in EPMT. (**M**) Time spent in open arms in the EPMT. (**N**) Latency to initiate feeding in NSFT. (**O**) Food consumption in NSFT. All data represent the mean ± SEM ($n = 8–10$ mice per group). $^*p < 0.05$, $^{***}p < 0.001$ versus mCherry + CNO group; $^{\#}p < 0.05$, $^{\#\#\#}p < 0.001$ versus hM4Di + VEH group.

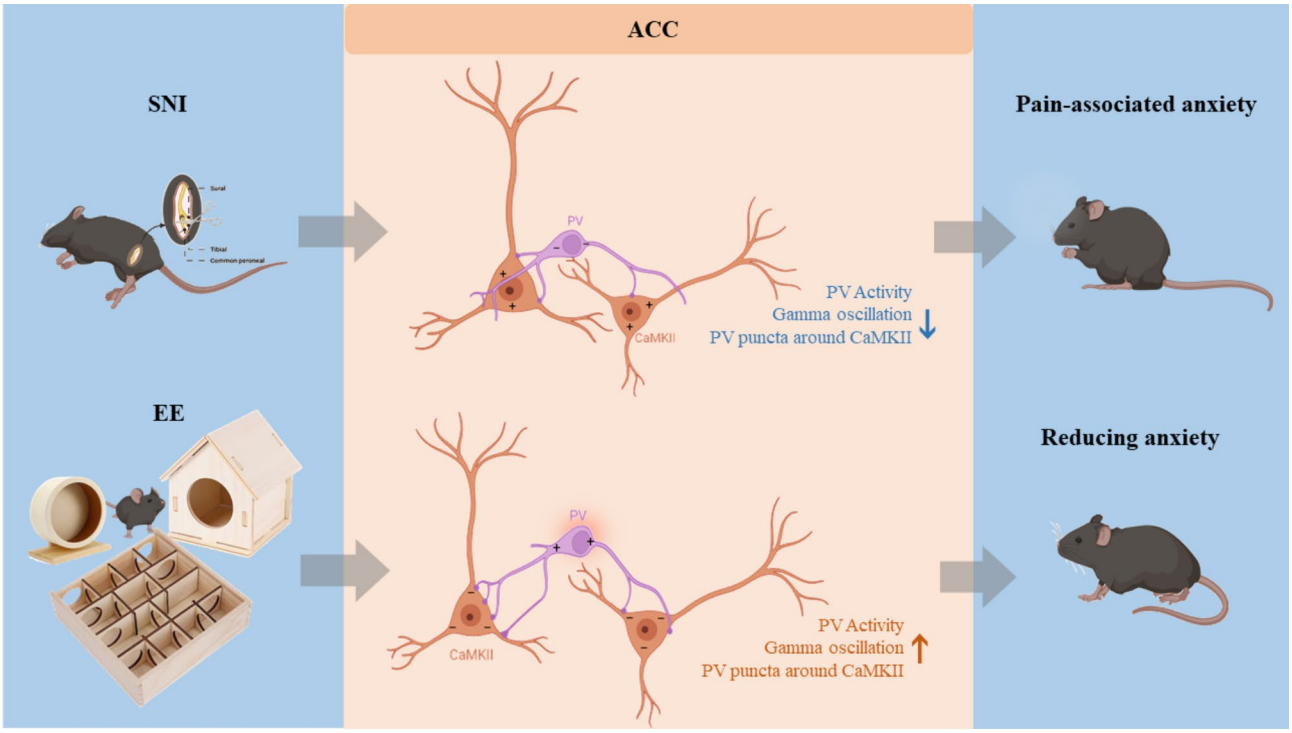

Fig. 7. A schematic diagram depicting EE affects neuropathic pain-related anxiety by regulating the function of PV interneurons in ACC. (Image created with Figdraw.com, with permission).

Data availability

The key data are contained in the figures, tables, and additional files. The datasets used or analyzed during this study can be further obtained from the corresponding author on reasonable request.

Received: 19 October 2024; Accepted: 19 March 2025
Published online: 24 March 2025

References

1. Finnerup, N. B., Kuner, R. & Jensen, T. S. Neuropathic pain: from mechanisms to treatment. *Physiol. Rev.* **101**(1), 259–301 (2021).
2. Feingold, D. et al. Problematic use of prescription opioids and medicinal cannabis among patients suffering from chronic pain. *Pain Med. (Malden Mass).* **18**(2), 294–306 (2017).
3. Zhuo, M. Neural mechanisms underlying anxiety-chronic pain interactions Trends *Neurosciences* **39**(3), 136–145 (2016).
4. Sztainberg, Y. & Chen, A. An environmental enrichment model for mice. *Nat. Protoc.* **5**(9), 1535–1539 (2010).
5. Toth, L. A. et al. Environmental enrichment of laboratory rodents: The answer depends on the question. *Comp. Med.* **61**(4), 314–321 (2011).
6. Zhang, Y. M. et al. Environmental enrichment reverses maternal sleep deprivation-induced anxiety-like behavior and cognitive impairment in CD-1 mice. *Front. Behav. Neurosci.* **16**, 943900 (2022).
7. Kim, K. et al. Reduced Interaction of Aggregated α-Synuclein and VAMP2 by Environmental Enrichment Alleviates Hyperactivity and Anxiety in a Model of Parkinson's Disease *Genes* **12**(3). (2021).
8. Keloglan Musuroglu, S. et al. Environmental enrichment as a strategy: Attenuates the anxiety and memory impairment in social isolation stress. *Int. J. Dev. Neuroscience: Official J. Int. Soc. Dev. Neurosci.* **82**(6), 499–512 (2022).

9. Wen, J. et al. The cAMP response element- binding protein/brain-derived neurotrophic factor pathway in anterior cingulate cortex regulates neuropathic pain and anxiodepression like behaviors in rats. *Front. Mol. Neurosci.* **15**, 831151 (2022).
10. Li, Y. D. et al. Anterior cingulate cortex projections to the dorsal medial striatum underlie insomnia associated with chronic pain. *Neuron* **112**(8). (2024).
11. Wang, T. Z. et al. Cingulate cGMP-dependent protein kinase I facilitates chronic pain and pain-related anxiety and depression. *Pain* **164**(11), 2447–2462 (2023).
12. Ren, D. et al. Anterior cingulate cortex mediates hyperalgesia and anxiety induced by chronic pancreatitis in rats. *Neurosci. Bull.* **38**(4), 342–358 (2022).
13. Hu, H., Gan, J. & Jonas, P. Interneurons. Fast-spiking, Parvalbumin⁺ GABAergic interneurons: From cellular design to microcircuit function. **345**, 1255263 (Science, 2014). 6196.
14. Li, H. et al. Loss of SST and PV positive interneurons in the ventral hippocampus results in anxiety-like behavior in 5xFAD mice. *Neurobiol. Aging* **117**, 165–178 (2022).
15. Page, C. E. et al. Prefrontal parvalbumin cells are sensitive to stress and mediate anxiety-related behaviors in female mice. *Sci. Rep.* **9**(1), 19772 (2019).
16. Xu, N. et al. Spared nerve injury increases the expression of microglia M1 markers in the prefrontal cortex of rats and provokes Depression-Like behaviors. *Front. NeuroSci.* **11**, 209 (2017).
17. Bonin, R. P., Bories, C. & De Koninck, Y. A simplified up-down method (SUDO) for measuring mechanical nociception in rodents using von Frey filaments. *Mol. Pain* **10**, 26 (2014).
18. Gonzalez-Cano, R. et al. Up-Down reader: an open source program for efficiently processing 50% von Frey thresholds. *Front. Pharmacol.* **9**, 433 (2018).
19. Ragu Varman, D. & Rajan, K. E. Environmental enrichment reduces anxiety by differentially activating serotonergic and neuropeptide Y (NPY)-Ergic system in Indian field mouse (Mus booduga): An Animal Model of Post-Traumatic Stress Disorder. *PloS One* **10**(5), e0127945 (2015).
20. Paxinos, G. F. & Franklin, K. *The Mouse Brain in Stereotaxic Coordinates* (Academic, 2003).
21. Wu, X. M. et al. Reduced Inhibition underlies early life LPS exposure induced-cognitive impairment: Prevention by environmental enrichment. *Int. Immunopharmacol.* **108**, 108724 (2022).
22. Vachon, P. et al. Alleviation of chronic neuropathic pain by environmental enrichment in mice well after the establishment of chronic pain. *Behav. Brain Functions: BBF* **9**, 22 (2013).
23. Kimura, L. F., Mattaraia, V. G. M. & Picolo, G. Distinct environmental enrichment protocols reduce anxiety but differentially modulate pain sensitivity in rats. *Behav. Brain. Res.* **364**, 442–446 (2019).
24. Estrázulas, M. et al. Central and peripheral effects of environmental enrichment in a mouse model of arthritis. *Int. Immunopharmacol.* **102**, 108386 (2022).
25. Zhao, M. M. et al. SynCAM1 Deficiency in the hippocampal parvalbumin interneurons contributes to sevoflurane-induced cognitive impairment in neonatal rats, **30**, e14554 (CNS Neuroscience & Therapeutics, 2024). 1.
26. Zugaib, J. et al. Glutamate/GABA balance in ACC modulates the nociceptive responses of vocalization: An expression of affective-motivational component of pain in guinea Pigs, **126** (Physiology & Behavior, 2014).
27. Kimura, L. F. et al. Early exposure to environmental enrichment protects male rats against neuropathic pain development after nerve injury. *Exp. Neurol.* **332**, 113390 (2020).
28. Gong, X. et al. Environmental enrichment reduces adolescent anxiety- and depression-like behaviors of rats subjected to infant nerve injury. *J. Neuroinflamm.* **15**(1), 262 (2018).
29. Shiers, S. et al. Neuropathic pain creates an enduring prefrontal cortex dysfunction corrected by the type II diabetic drug Metformin but not by Gabapentin. *J. Neuroscience: Official J. Soc. Neurosci.* **38**(33), 7337–7350 (2018).
30. Shao, F. et al. Electroacupuncture ameliorates chronic inflammatory Pain-Related anxiety by activating PV interneurons in the anterior cingulate cortex. *Front. Neurosci.* **15**, 691931 (2021).
31. Li, Y. D. et al. Anterior cingulate cortex projections to the dorsal medial striatum underlie insomnia associated with chronic pain. *Neuron* **112**(8), 1328–1341e4 (2024).
32. Zhu, D. Y. et al. The increased in vivo firing of pyramidal cells but not interneurons in the anterior cingulate cortex after neuropathic pain. *Mol. Brain*. **15**(1), 12 (2022).
33. Cardin, J. A. et al. Driving fast-spiking cells induces gamma rhythm and controls sensory responses. *Nature* **459**(7247), 663–667 (2009).
34. Zhang, Z. G. et al. Gamma-band oscillations in the primary somatosensory cortex–a direct and obligatory correlate of subjective pain intensity. *J. Neurosci.* **32**(22), 7429–7438 (2012).
35. Li, Z. et al. Gamma-band oscillations of pain and nociception: A systematic review and meta-analysis of human and rodent studies. *Neurosci. Biobehav Rev.* **146**, 105062 (2023).
36. Han, C. et al. Multiple gamma rhythms carry distinct Spatial frequency information in primary visual cortex. *PLoS Biol.* **19**(12), e3001466 (2021).
37. Mably, A. J. & Colgin, L. L. Gamma oscillations in cognitive disorders. *Curr. Opin. Neurobiol.* **52**, 182–187 (2018).
38. Sun, X. R. et al. Amelioration of oxidative stress-induced phenotype loss of parvalbumin interneurons might contribute to the beneficial effects of environmental enrichment in a rat model of post-traumatic stress disorder. *Behav. Brain Res.* **312**, 84–92 (2016).
39. Inácio, A. R., Ruscher, K. & Wieloch, T. Enriched environment downregulates macrophage migration inhibitory factor and increases parvalbumin in the brain following experimental stroke. *Neurobiol. Dis.* **41**(2), 270–278 (2011).
40. Irie, K. et al. An enriched environment ameliorates the reduction of parvalbumin-positive interneurons in the medial prefrontal cortex caused by maternal separation early in life. *Front. Neurosci.* **17**, 1308368 (2023).
41. Cichon, J. et al. Activation of cortical somatostatin interneurons prevents the development of neuropathic pain. *Nat. Neurosci.* **20**(8), 1122–1132 (2017).
42. Beierlein, M., Gibson, J. R. & Connors, B. W. Two dynamically distinct inhibitory networks in layer 4 of the neocortex. *J. Neurophysiol.* **90**(5), 2987–3000 (2003).
43. Urban-Ciecko, J. & Barth, A. L. Somatostatin-expressing neurons in cortical networks. *Nat. Rev. Neurosci.* **17**(7), 401–409 (2016).
44. Yang, J. X. et al. Caveolin-1 in the anterior cingulate cortex modulates chronic neuropathic pain via regulation of NMDA receptor 2B subunit. *J. Neuroscience: Official J. Soc. Neurosci.* **35**(1), 36–52 (2015).
45. Li, X. H. et al. Oxytocin in the anterior cingulate cortex attenuates neuropathic pain and emotional anxiety by inhibiting presynaptic long-term potentiation. *Cell. Rep.* **36**(3), 109411 (2021).
46. Li, K. et al. Distinct ventral hippocampal inhibitory microcircuits regulating anxiety and fear behaviors. *Nat. Commun.* **15**(1), 8228 (2024).
47. Babaev, O. et al. IgSF9b regulates anxiety behaviors through effects on centromedial amygdala inhibitory synapses. *Nat. Commun.* **9**(1), 5400 (2018).
48. Sun, L. et al. Parabrachial nucleus circuit governs neuropathic pain-like behavior. *Nat. Commun.* **11**(1), 5974 (2020).
49. Yalcin, I. et al. A time-dependent history of mood disorders in a murine model of neuropathic pain. *Biol. Psychiatry* **70**(10), 946–953 (2011).

Author contributions
Y.J.J. and Z.G.F. designed and supervised the study. R.Z.Y. and H.B.Y. performed the experiment and wrote the main manuscript text. Z.L.Y. and L.X.J. participated in analyzing the results. T.Y.X. edited and revised the manuscript. All authors reviewed and approved the final manuscript.

Funding
The study was supported by The Programme of Introducing Talents of Discipline to Universities of Henan: Anesthesia and Brain Research (No. CXJD2019008), National Natural Science Foundation of China (82371279 to GFZ) and the National Natural Science Foundation of China (82401461).

Declarations

Competing interests
The authors declare no competing interests.

Ethics approval
All experiment received approval from the Animal Care and Welfare Committee of Zhengzhou University.

Additional information
Correspondence and requests for materials should be addressed to G.-F.Z. or J.-J.Y.

Reprints and permissions information is available at www.nature.com/reprints.

Publisher's note Springer Nature remains neutral with regard to jurisdictional claims in published maps and institutional affiliations.